Preprint typeset using LaTeX style emulateapj v. 5/2/11

HIGH ENERGY NEUTRINO AND GAMMA-RAY TRANSIENTS FROM RELATIVISTIC SUPERNOVA SHOCK BREAKOUTS

Kazumi Kashiyama[1], Kohta Murase[2,3], Shunsaku Horiuchi[2,4], Shan Gao[1], and Peter Mészáros[1]

ABSTRACT

Relativistic shocks that accompany supernovae (SNe) produce X-ray burst emissions as they break out in the dense circumstellar medium around the progenitors. This phenomenon is sometimes associated with peculiar low-luminosity gamma-ray bursts (LL GRBs). Here, we investigate the high energy neutrino and gamma-ray counterparts of such a class of SNe. Just beyond the shock breakout radius, particle acceleration in the collisionless shock starts to operate in the presence of breakout photons. We show that protons may be accelerated to sufficiently high energies and produce high energy neutrinos and gamma rays via the photomeson interaction. These neutrinos and gamma rays may be detectable from $\lesssim 10$ Mpc away by IceCube/KM3Net as multi-TeV transients almost simultaneously with the X-ray burst emission, and even from $\lesssim 100$ Mpc away with follow-up observations by CTA using a wide-field sky monitor like *Swift* as a trigger. A statistical technique using a stacking approach could also be possible for the detection, with the aid of the SN optical/infrared counterparts. Such multi-messenger observations offer the possibility to probe the transition of relativistic shocks from radiation-mediated to collisionless ones, and would also constrain the mechanisms of particle acceleration and emission in LL GRBs.

Subject headings: acceleration of particles — neutrinos — shock waves — supernovae:general

1. INTRODUCTION

There is increasing evidence for a class of supernovae (SNe) which are accompanied by relativistic shocks ($\beta_{\rm sh} \gtrsim 0.1$). These are initially radiation mediated while going through optically thick gas, *i.e.,* the stellar or a circumstellar envelope (Weaver 1976). The typical photon energy could be as high as 10-100 keV within a few Thomson mean free paths near the shock (e.g., Katz et al. 2010; Budnik et al. 2010). Once the optical depth becomes small enough that the photon diffusion velocity is similar to the shock velocity, photons begin to escape and are observed as the shock breakout emission. The energy spectrum is expected to be a combination of non-thermal and quasi-thermal (e.g., Wang et al. 2007; Waxman et al. 2007; Nakar & Sari 2010; Chevalier & Irwin 2012). Such X-ray breakouts have now been confirmed in some cases (Soderberg et al. 2008; Ofek et al. 2012).

An interesting application of relativistic shock breakouts is to low luminosity gamma-ray bursts (LL GRBs) associated with SNe, such as GRB060218/SN2006aj (Campana et al. 2006; Soderberg et al. 2006) and GRB100316D/SN2010bh (Chornock et al. 2010; Starling et al. 2011). These GRBs share peculiar characteristics compared to typical long GRBs: smaller luminosities ($L_{\rm iso,\gamma} \sim 10^{46}$ erg/s), softer peak energies ($\varepsilon_{\rm peak} \sim$ 1-10 keV), and longer durations ($t_\gamma \sim 1000$ sec). The relativistic shock breakout model can explain these characteristics (Soderberg et al. 2006) [5] although a more detailed modeling is necessary for the energy spectrum (Ghisellini et al. 2007). The host galaxies are both nearby ($z = 0.0331$ for GRB060218 (Mirabal et al. 2006) and $z = 0.059$ for GRB100316D (Vergani et al. 2010)). The dimness and the proximity indicate that there might be a considerable number of sub-threshold events resulting in a relatively high local rate of some $R_{\rm LL}(z = 0) \lesssim 500$ Gpc^{-3}yr^{-1} (Guetta & Della Valle 2007; Liang et al. 2007). Hence LL GRBs may be one of the most promising targets for ongoing and upcoming multi-messenger astronomy searches (Ando et al. 2012), e.g. with specially designed facilities such as AMON[6].

In general, shocks would become collisionless beyond the breakout radii, allowing charged particles to be accelerated (Murase et al. 2011; Katz et al. 2011). The accelerated protons can then produce mesons by the photomeson interaction or the inelastic *pp* reaction, resulting in neutrinos and gamma rays as decay products of the mesons. This situation is analogous to the photospheric scenario of GRB prompt emission (Murase 2008; Wang & Dai 2009; Gao et al. 2012). By detecting these signals simultaneously with the breakout emission, one can probe the evolution of shocks converting from the radiation mediated to the collisionless regime, and investigate the baryon acceleration there.

In this *Letter*, we evaluate the high energy neutrino and gamma-ray emission from relativistic shocks breaking out. We are primarily concerned with the application to LL GRBs associated SNe, but our prescriptions can be generally applied to other situations, e.g., ordinary (non-GRB) Ibc SN shocks breaking out of the progenitor, by appropriately scaling the velocity and the breakout ra-

kzk15@psu.edu
[1] Department of Astronomy & Astrophysics; Department of Physics; Center for Particle & Gravitational Astrophysics; Pennsylvania State University, University Park, PA 16802
[2] CCAPP & Department of Physics, Ohio State University, 191 W. Woodruff Ave., Columbus, Ohio 43210
[3] Hubble Fellow, School of Natural Sciences, Institute for Advanced Study, 1 Einstein Dr. Princeton NJ 08540
[4] Center for Cosmology, Department of Physics and Astronomy, University of California, Irvine, CA 92697-4575, USA

[5] Mazzali et al. (2006) and Toma et al. (2007) proposed strongly magnetized neutron stars, instead of black holes, as the central engine to explain the characteristics (see also Fan et al. 2011).
[6] http://amon.gravity.psu.edu/

dius of the shock.

Our work differs from previous studies (Murase et al. 2006; Gupta & Zhang 2007) where neutrino counterparts of LL GRBs were evaluated based on the *relativistic* jet model ($\Gamma_{\rm j} \gg 1$), which is also viable (Toma et al. 2007; Ghisellini et al. 2007). Although the main microphysical process, *i.e.* the photomeson interaction between accelerated protons and the observed X-ray photons, is the same, the predictions are not the same, due to differences in the emission radius and the Lorentz factor (Katz et al. 2011). Also, our prediction on the detectability of the gamma-ray counterpart is more positive than the previous estimate. The present results also differ from those of Murase et al. (2011), which considered the neutrino and gamma-ray emission from *non-relativistic* shocks ($\beta_{\rm sh} \lesssim 0.01$) colliding with the dense circumstellar material

2. MODEL SET-UP

Our main parameters are the shock velocity $\beta_{\rm sh}$ and the shock breakout radius $r_{\rm sb}$, where the optical depth ahead of the shock becomes as small as $\approx 1/\beta_{\rm sh}$. The duration of the breakout X-ray emission is comparable to the dynamical time scale,

$$t_\gamma \approx t_{\rm dyn} \approx \frac{r_{\rm sb}}{\beta_{\rm sh} c} \sim 2.0\times10^3\ r_{\rm sb,13.8}{\beta_{\rm sh}}^{-1}\ {\rm sec}. \quad (1)$$

The intrinsic energy budget can be estimated as $\mathcal{E}_{\rm iso} \approx 4\pi(1/2)\rho {r_{\rm sb}}^2 l_{\rm T} {\beta_{\rm sh}}^2 c^2$, or

$$\mathcal{E}_{\rm iso} \sim 5.1\times10^{49}\ {r_{\rm sb,13.8}}^2\beta_{\rm sh}\ {\rm erg}. \quad (2)$$

Here $l_{\rm T}$ and $\sigma_{\rm T}$ are the mean free path and the cross section of the Thomson scattering, and we use the relation at the shock breakout radius, $l_{\rm T} \approx r_{\rm sb} \approx m_{\rm p}/\sigma_{\rm T}\rho\beta_{\rm sh}$. The mean photon luminosity is then $L_{{\rm iso},\gamma} \sim \epsilon_\gamma \mathcal{E}_{\rm iso}/t_\gamma$, or

$$L_{{\rm iso},\gamma} \sim 2.6\times10^{46}\ \epsilon_\gamma r_{\rm sb,13.8}\beta_{\rm sh}^2\ {\rm erg/sec}, \quad (3)$$

where ϵ_γ is the fraction of the energy delivered to radiation. We assume that the prompt X-ray emission of GRB060218- and GRB100316D-like events is due to the shock breakout emission, and set $\beta_{\rm sh} = 1$ and $r_{\rm sb} = 6.0\times10^{13}$ cm as the fiducial values which roughly reproduce the observed characteristics.

It is difficult to evaluate the time-dependent energy spectrum of the photon field in-situ around the shock breakout radius (Nakar & Sari 2010; Chevalier & Irwin 2012). Here, we substitute instead the observed spectrum which, over most of the prompt emission episode, can be fitted approximately by a broken power law, $dn/d\varepsilon = n_{\rm b}(\varepsilon/\varepsilon_{\rm b})^{-\alpha}$ for $\varepsilon_{\rm min} < \varepsilon < \varepsilon_{\rm b}$, and $dn/d\varepsilon = n_{\rm b}(\varepsilon/\varepsilon_{\rm b})^{-\beta}$ for $\varepsilon_{\rm b} < \varepsilon < \varepsilon_{\rm max}$. [7] We set $\alpha = 1.42$, $\beta = 2.48$, $\varepsilon_{\rm b} = 16$ keV and $L^b_{{\rm iso},\gamma}$ that is the luminosity at $\varepsilon_{\rm b}$, following the observation of GRB100316D (Fan et al. 2011). Note that $L^b_{{\rm iso},\gamma}$ can be related to $L_{{\rm iso},\gamma}$ via $U_\gamma \equiv \int_{\varepsilon_{\rm min}}^{\varepsilon_{\rm max}} \varepsilon(dn/d\varepsilon)d\varepsilon = L_{{\rm iso},\gamma}/4\pi {r_{\rm sb}}^2 c$. The low energy cut-off is assumed to be $\varepsilon_{\rm min} = 1.0$ keV where the observed SED declines sharply. In fact, *Swift* UVOT identified a prompt UV-optical emission with a photon index harder than 3/2 for GRB060218 (Ghisellini et al. 2007), and gave only an upper limit for GRB100316D (Starling et al. 2011). These soft photons can affect the opacity of high energy gamma rays, as we show below. The high energy cut-off can be set as $\varepsilon_{\rm max} = 1.0$ MeV since the pair absorption would be crucial above this energy.

The mass density of the circumstellar medium at the shock breakout radius can be evaluated as

$$\rho \approx \frac{m_{\rm p}}{\sigma_{\rm T} r_{\rm sb}\beta_{\rm sh}} \sim 4.2\times10^{-14}\ {r_{\rm sb,13.8}}^{-1}{\beta_{\rm sh}}^{-1}\ {\rm g/cm^3}. \quad (4)$$

If the matter is provided by a stellar wind where $\rho \approx \dot{M}/4\pi v_{\rm w} {r_{\rm sb}}^2$, the mass ejection rate may be as large as $\dot{M} \sim 0.03\ v_{\rm w,9} r_{\rm sb,13.8}{\beta_{\rm sh}}^{-1}\ M_\odot/{\rm yr}$ for a wind velocity $v_{\rm w} \sim 10^9\ v_{\rm w,9}$ cm/s. Such massive winds in the pre-collapse phase have been inferred especially for type IIn SN progenitors (Smith et al. 2010; Stoll et al. 2011; Chandra et al. 2012a,b; Roming et al. 2012), and, in some cases, the shock breakout X-ray photons have been observed (Ofek et al. 2012).

3. PROTON ACCELERATION

Beyond the breakout radius, the shock can no longer be mediated by the radiation. However, electromagnetic fields amplified by plasma instabilities will determine the shock structure, *i.e.* the shock becomes collisionless (Murase et al. 2011; Katz et al. 2011). The magnetic field strength can be estimated as $B \approx (8\pi\xi_{\rm B}U_\gamma)^{1/2} \sim 9.6\times10^4\ (\xi_{\rm B}/0.1)^{1/2} {r_{\rm sb,13.8}}^{-1/2}\beta_{\rm sh}$ G, where $\xi_{\rm B} \equiv U_{\rm B}/U_\gamma$ represents the magnetic field amplification efficiency. A fraction of the protons can be accelerated into a non-thermal distribution by the first order Fermi process as they repeatedly cross the shock. The maximum energy of the protons is determined by the condition, $t_{\rm acc} \le t_{\rm p}$, where $t_{\rm acc} = \eta E_{\rm p}/eBc$ is the acceleration time (in the Bohm diffusion limit, $\eta \sim 2\pi$), and ${t_{\rm p}}^{-1} \equiv {t_{\rm ad}}^{-1} + {t_{\rm syn}}^{-1} + {t_{\rm IC}}^{-1} + {t_{\rm BH}}^{-1} + {t_{\rm p\gamma}}^{-1} + {t_{\rm pp}}^{-1}$ is the total energy loss time scale, including the effect of the adiabatic expansion (ad), the synchrotron radiation (syn), inverse Compton radiation (IC), the Bethe-Heitler type interactions (BH), the photo meson interactions (pγ), and the inelastic pp collisions (pp). Fig.1 shows the proton energy versus the various time scales, obtained with the calculation codes used in Murase (2008). One can see that the synchrotron cooling time $t_{\rm syn} = (3{m_{\rm p}}^4 c^3/4\sigma_{\rm T}{m_{\rm e}}^2){U_{\rm B}}^{-1}{E_{\rm p}}^{-1}$ is the most important for the proton maximum energy. The condition $t_{\rm acc} \lesssim t_{\rm syn}$ appropriately gives

$$E_{\rm p} \lesssim 6.3\ \left(\frac{\xi_{\rm B}}{0.1}\right)^{-1/4}\left(\frac{\eta}{2\pi}\right)^{-1/2} {r_{\rm sb,13.8}}^{1/4}{\beta_{\rm sh}}^{-1/2}\ {\rm EeV}, \quad (5)$$

and protons can be accelerated up to $\sim$ EeV energies. We assume a power law distribution of the protons, $dN/dE_{\rm p} \propto E_{\rm p}^{-2}$. The normalization is determined by introducing the acceleration efficiency, $\epsilon_{\rm CR} \equiv \mathcal{E}_{\rm CR}/\mathcal{E}_{\rm iso}$. Here $\mathcal{E}_{\rm CR} \equiv \int_{E_{\rm p,min}}^{E_{\rm p,max}} E_{\rm p}(dN/dE_{\rm p})dE_{\rm p}$ is the total energy of the non-thermal protons. We set $E_{\rm p,min} = 1$GeV, and $E_{\rm p,max}$ is given by Eq.(5).

4. NEUTRINO AND GAMMA-RAY EMISSION

[7] We have confirmed that the following arguments and results do not change dramatically if we substitute a blackbody like spectrum.

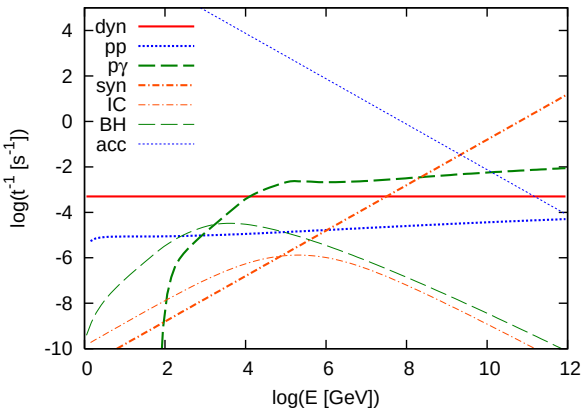

FIG. 1.— Acceleration time scale and various cooling time scales of protons for a relativistic shock breakout with $\beta_{\rm sh} = 1.0$, $r_{\rm sb} = 6 \times 10^{13}$cm. For the breakout photons, we assume a broken power low with a bolometric luminosity $L^b_{{\rm iso},\gamma} = 10^{46}$ erg/sec as explained in the text. We also set $\xi_{\rm B} = 0.1$, and $\eta = 2\pi$.

We consider the neutrinos and the gamma rays from the decay of mesons generated by both the photomeson production and inelastic pp reaction. In the analytical estimate below, we only discuss pions which turn out to give a dominant contribution. But the contribution from kaon decay is numerically included as in Murase (2008).

We can estimate the fraction of energy transferred from the non-thermal protons to the pions by the photomeson interactions as $\min[1, f_{\rm p\gamma}]$ where $f_{\rm p\gamma} \equiv t_{\rm dyn}/t_{\rm p\gamma}$. Using the rectangular approximation (Waxman & Bahcall 1997) for a photon spectrum approximated as a broken power law, we have

$$f_{\rm p\gamma} \sim \epsilon_\gamma {\varepsilon_{\rm b,16keV}}^{-1} \beta_{\rm sh} \times \begin{cases} (E_{\rm p}/E_{\rm p,b})^{\beta-1} & (E_{\rm p} < E_{\rm p,b}), \\ (E_{\rm p}/E_{\rm p,b})^{\alpha-1} & (E_{\rm p,b} < E_{\rm p}), \end{cases} \quad (6)$$

where $E_{\rm p,b} = 0.5\ \bar{\varepsilon} {\varepsilon_{\rm b}}^{-1} m_{\rm p} c^2 \sim 8.8\ {\varepsilon_{\rm b,16keV}}^{-1}$ TeV with $\bar{\varepsilon} \sim 0.34$ GeV. The multi-pion production becomes dominant above $\approx 0.5\ \bar{\varepsilon} {\varepsilon_{\rm min}}^{-1} m_{\rm p} c^2 \sim 140\ {\varepsilon_{\rm min,keV}}^{-1}$ TeV (cf. Murase et al. 2008). We can conclude that a significant fraction of non-thermal protons with energies 10 TeV $\lesssim E_{\rm p} \lesssim$ EeV will be converted into pions.

The inelastic pp cooling time is ${t_{\rm pp}}^{-1} \approx (\rho/m_{\rm p}) \kappa_{\rm pp} \sigma_{\rm pp} c$. The fraction of energy an incident proton loses, $f_{\rm pp} \equiv t_{\rm dyn}/t_{\rm pp}$, can be evaluated as

$$f_{\rm pp} \sim 0.03\ {\beta_{\rm sh}}^{-2}, \quad (7)$$

where we use approximately constant values for the inelasticity $\kappa_{\rm pp} \sim 0.5$ and for the cross section $\sigma_{\rm pp} \sim 4 \times 10^{-26}$ cm^2, appropriate at high energies. Eq.(7) indicates that the inelastic pp collisions can also contribute moderately to the pion production as in the case of GRB photospheric emissions.

Neutrino Emission.- Neutrinos are mainly produced as decay products of charged pions. One can find that the charged pions with $E_\pi \gtrsim 2.7\ (\xi_{\rm B}/0.1)^{-1/2} {\epsilon_\gamma}^{-1/2} {r_{\rm sb,13.8}}^{1/2} {\beta_{\rm sh}}^{-1}$ PeV will lose their energy before decaying due to the synchrotron cooling. Given that the resultant neutrinos have typically $\sim 1/4$ of the parent pion energy, one expects TeV-PeV neutrinos. The peak fluence from a single supernova/burst event can be analytically estimated as

$${E_\nu}^2 \phi_\nu \approx (1/4\pi D_{\rm L}^2) \times (1/4) \min[1, f_{\rm p\gamma}] ({E_{\rm p}}^2 dN/dE_{\rm p}), \text{ or}$$

$${E_\nu}^2 \phi_\nu \sim 10^{-5} \left(\frac{D_{\rm L}}{10{\rm Mpc}}\right)^{-2} \frac{\epsilon_{\rm CR}}{0.1} f_{\rm p\gamma} {r_{\rm sb,13.8}}^2 \beta_{\rm sh}\ {\rm erg/cm^2}, \quad (8)$$

where $D_{\rm L}$ is the luminosity distance to the source.

Fig.2 shows the energy fluences of neutrinos obtained numerically using the calculation codes of Murase (2008), for the same parameters as Fig.1. The dashed and dotted lines show the contribution from the photomeson and inelastic pp interactions, respectively. We have verified that contributions from the kaon decay become important only above $\sim$ 10 PeV. The signal is well above the zenith-angle-averaged atmospheric neutrino background (ANB, dotted-dash lines; thick one for $t_\gamma \sim 2 \times 10^3$ sec, and thin one for 1 day). The number of muon events due to the muon neutrinos above TeV energies can be estimated as $N_\mu \sim 0.2\ (\epsilon_{\rm CR}/0.2)(D_{\rm L}/10{\rm Mpc})^{-2} {r_{\rm sb,13.8}}^2 \beta_{\rm sh}$ using IceCube/KM3net (Karle & for the IceCube Collaboration 2010; Katz 2006). Based on our fiducial parameters, IceCube/KM3net can marginally detect a nearby source at $\lesssim$ 10 Mpc, although such events occur very rarely *i.e.*, $\lesssim 0.002$ yr^{-1} for a local LL GRB event rate $R_{\rm LL}(z = 0) \sim 500$ Gpc^{-3}yr^{-1} (Guetta & Della Valle 2007).

From Fig.2, one can see that the typical neutrino energy in the relativistic shock breakout model is TeV-PeV. By comparison, the relativistic jet models of LL GRBs predict relatively higher energy PeV-EeV neutrinos (Murase et al. 2006; Gupta & Zhang 2007). This difference is mainly because the shock breakout model involves a lower Lorentz factor and a stronger cooling of mesons. In a relativistic jet, the peak photon energy in the comoving frame is $\varepsilon'_{\rm b} = \varepsilon_{\rm b}/\Gamma_{\rm j}$, where $\Gamma_{\rm j}$ is the Lorentz factor of the jet. The typical energy of protons interacting with photons via the photomeson production is ${E_{\rm p}}' \sim 0.5\ \bar{\varepsilon} {\varepsilon_{\rm b}}'^{-1} m_{\rm p} c^2$. The resultant neutrino energy will be $E_\nu \sim 0.05 \times {E_{\rm p}}' \Gamma_{\rm j}$ in the observer frame, which is 100 $(\Gamma_{\rm j}/10)^2$ times larger than our model. Thus, high-energy neutrino observations can provide clues to the emission model of LL GRBs.

In principle, the shock velocity could be independently constrained through the neutrino spectroscopy. From Eq.(6) and (7), both $f_{\rm p\gamma}$ and $f_{\rm pp}$ are present irrespective of $r_{\rm sb}$, and only depend on $\beta_{\rm sh}$. The relative importance of photomeson to inelastic pp collisions directly affects the neutrino energy spectrum. In the case of relativistic shocks with $\beta_{\rm sh} \gtrsim 0.1$, the spectrum will have a bumpy structure like Fig.2. On the other hand, slower shocks will produce relatively flat spectra because of efficient inelastic pp interactions (see e.g., Murase et al. (2011)).

Gamma-ray counterparts.- Gamma rays are mainly injected by neutral meson decays. Since the neutral mesons do not suffer synchrotron cooling, the maximum energy of gamma rays can be as high as $\sim$ 10% of the parent protons, that is $\sim$ 100 PeV in our fiducial case. At high energies above $\sim$ MeV, the electron-positron pair production can attenuate the gamma-ray flux. In the emission region, we can roughly take into account the attenuation by $\approx 1/(1 + \tau_{\gamma\gamma})$, where $\tau_{\gamma\gamma}$ is the electron-positron pair production optical depth (e.g., Baring 2006). The observed photon spectrum of GRB100316D is employed to calculate the optical depth

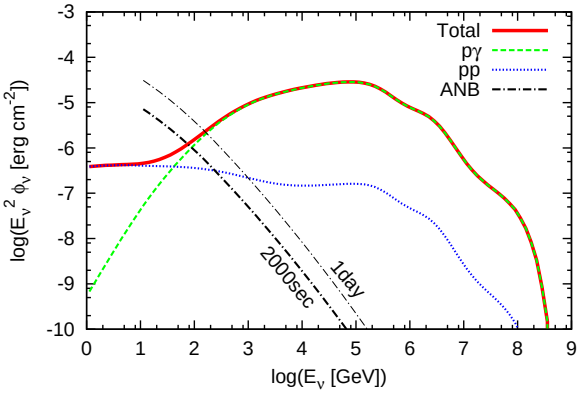

FIG. 2.— Energy fluences of neutrinos from a relativistic shock breakout using the same parameters as Fig.1. We set $\epsilon_{\rm CR} = 0.2$ and $D_{\rm L} = 10$ Mpc. Lines represent a contribution from the photomeson production (dashed), the inelastic pp reaction (dotted), and the total (solid). The dotted-dashed lines show the zenith-angle averaged atmospheric neutrino background (ANB) within a circle of deg for $\Delta t = 2.0 \times 10^3$ sec (thick) and $\Delta t = 1$ day (thin).

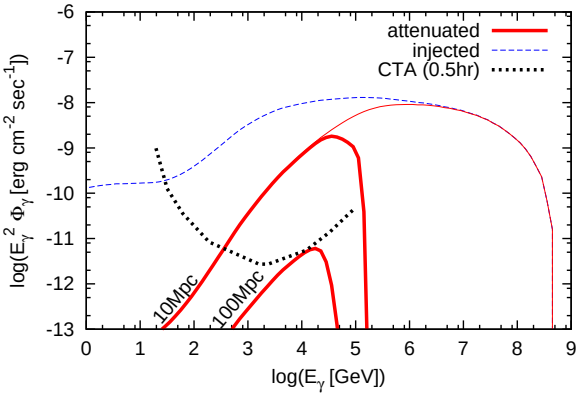

FIG. 3.— Energy fluxes of gamma rays corresponding to Fig.2. The emission duration is equal to that of X rays; $t_\gamma = 2.0 \times 10^3$ sec. We show the cases of $D_{\rm L} = 10$ and 100 Mpc (thick solid lines). For the former, we also show the injected spectrum without attenuation (dashed line) and only including attenuation within the emission region (thin line). The dotted line shows 0.5 hr $= 1.8 \times 10^3$ sec differential sensitivity of CTA for a 5σ detection.

of the emission region numerically, with a Rayleigh-Jeans tail below $\varepsilon_{\rm min} = 1$ keV. This would be reasonable, since the result is not affected much as long as the photon index there is harder than 1. Note that the gamma-ray attenuation on matter due to the Bethe-Heitler pair production is not important in the case of relativistic shock breakouts. The optical depth can be roughly estimated as $\tau_{\rm BH} \approx (1/137)\sigma_{\rm T}(\rho/m_{\rm p})r_{\rm sb} \sim 0.0074\ \beta_{\rm sh}^{-1}$. This can be important in the case of non-relativistic shocks with $\beta_{\rm sh} \lesssim 0.01$ (e.g., Murase et al. 2011). We also take into account the attenuation by the extragalactic background light (EBL; Kneiske et al. 2004).

Fig.3 shows the numerically calculated energy spectrum of gamma rays. The thick solid line represents the expected flux from a single LL GRB event at 10 Mpc and 100 Mpc. The emission duration is set to that of the X rays, $t_\gamma \sim 2.0 \times 10^3\ r_{\rm sb,13.8}\beta_{\rm sh}{}^{-1}$ sec. As a reference, we also show the injected spectrum without attenuation (dashed line) and only including the attenuation within the emission region (thin solid line) for the 10 Mpc case. It can be seen that the attenuation of GeV $\lesssim E_\gamma \lesssim 100$ TeV gamma rays is mainly due to the photon field in the emission region below/around $\varepsilon \gtrsim 1$ keV. In our case, the attenuation rate decreases with the energy because of the Klein-Nishina suppression. On the other hand, gamma rays above ~ 100 TeV are mostly attenuated by the EBL. In Fig.3, we also show the differential sensitivity of CTA for a 5σ detection with an exposure time comparable to t_γ, 0.5hr $= 1.8 \times 10^3$ sec (dotted line; Actis et al. 2011). One can see that CTA can detect the multi-TeV gamma rays even from 100 Mpc, within which the all-sky event rate would be $\sim 2\ {\rm yr}^{-1}$ for $R_{\rm LL}(z=0) \sim 500\ {\rm Gpc}^{-3}{\rm yr}^{-1}$. The FOV of CTA with the shown sensitivity ~ 5 deg would not be wide enough for a blind search. On the other hand, a survey mode with a wider FOV would not be sensitive enough to detect the signal. Thus, for CTA, a rapid follow-up observation triggered by a wide-field X-ray telescope such as *Swift* or a *Lobster*-type instrument is needed. Assuming that the sky coverage is $\gtrsim 10\%$, one can expect $\gtrsim 0.2$ events ${\rm yr}^{-1}$ within 100 Mpc. The detection rate would be increased by a simultaneous operation of HAWC with a sensitivity $\sim 10^{-10}$erg cm^{-2}sec^{-1} for ~ 100 TeV gamma rays (DeYoung & HAWC Collaboration 2012).

A detection of the multi-TeV gamma-ray transient, as expected in this model, would also constrain the emission mechanism of LL GRB. This is in contrast to the relativistic jet model, where as in the neutrino counterpart, the typical energy of the gamma rays injected by the photomeson reaction would be $\gtrsim$ PeV, which will be completely attenuated by the EBL even if they can escape the emission region.

5. SUMMARY AND DISCUSSION

We have shown that relativistic shock breakouts in SNe can be accompanied by multi-TeV neutrino and gamma-ray transients. These can provide diagnostics for a radiation mediated shock converting into a collisionless shock, and for baryon acceleration there. We can also get clues to the emission mechanism of LL GRBs by detecting such high energy counterparts simultaneously with the prompt X-ray emission. The multi-TeV gamma rays can be detectable even from 100 Mpc away using CTA. These results motivate follow-up observations triggered by a wide-field X-ray telescope like *Swift*.

While typically one expects very few neutrino events from those relativistic SNe, nevertheless searches for them would be aided by other possible counterparts. Using the information of optical/infrared counterparts of core-collapse SNe, one can essentially fix the target position within the angular resolution of IceCube/KM3net $\lesssim$ deg, and also restrict the time domain of the neutrino search within $\sim$ day. The atmospheric neutrino background (ANB) of IceCube/KM3net within a circle of a degree over a day is roughly $\lesssim 10^{-5}\ E_{\nu,100{\rm TeV}}{}^{-2}$ events day^{-1}. In terms of this ANB flux, neutrinos from relativistic shock breakouts within $D_{\rm L} \sim E_{\nu,100{\rm TeV}}$ Gpc can give a signal-to-noise ratio $\gtrsim 1$ (see also Fig.2). One could then statistically extract $O(1)$ astrophysical neutrinos by stacking the optical counterparts of $O(10^5)$ SNe within $z \lesssim 0.3$, whether or not the X-ray counterparts are observed. Given that the whole sky event rate of such LL GRBs would be $\sim 3 \times 10^4\ {\rm yr}^{-1}$ assuming $R_{\rm LL}(z=0) \sim 500\ {\rm Gpc}^{-3}{\rm yr}^{-1}$, a decadal SNe search

up to $z \lesssim 0.3$ with a sky coverage $\gtrsim 10\%$ is needed While still a challenging task, this kind of astronomy may be possible in the up-coming LSST era (Lien & Fields 2009).

Ordinary SNe Ibc can also be accompanied by relativistic shocks with $\beta_{\rm sh} \gtrsim 0.1$, which inevitably break out at a certain radius and produce neutrinos in a similar manner similar as discussed above. Although the typical fraction of the energy in the relativistic component would be relatively small, $\mathcal{E}_{\rm iso} \lesssim 10^{48}$ erg (e.g., Soderberg et al. 2010), the event rate is much larger than for LL GRBs, $R_{\rm Ibc}(z=0) \sim 2 \times 10^4$ Gpc^{-3}yr^{-1} (Madau et al. 1998). Thus, they would give a comparable or a larger amounts of neutrinos by using the above stacking method.

We thank Bin-Bin Zhang and Peter Veres for valuable discussions. This work is supported in part by a JSPS fellowship for research abroad, by NSF PHY-0757155 and the CCAPP workshop on "Revealing Deaths of Massive Stars with GeV-TeV Neutrinos".

REFERENCES

Actis, M., Agnetta, G., Aharonian, F., et al. 2011, Experimental Astronomy, 32, 193
Ando, S., Baret, B., Bouhou, B., et al. 2012, ArXiv e-prints
Baring, M. G. 2006, ApJ, 650, 1004
Budnik, R., Katz, B., Sagiv, A., & Waxman, E. 2010, ApJ, 725, 63
Campana, S., Mangano, V., Blustin, A. J., et al. 2006, Nature, 442, 1008
Chandra, P., Chevalier, R. A., Chugai, N., et al. 2012a, ApJ, 755, 110
Chandra, P., Chevalier, R. A., Irwin, C. M., et al. 2012b, ApJ, 750, L2
Chevalier, R. A., & Irwin, C. M. 2012, ApJ, 747, L17
Chornock, R., Berger, E., Levesque, E. M., et al. 2010, ArXiv e-prints
DeYoung, T., & HAWC Collaboration. 2012, Nuclear Instruments and Methods in Physics Research A, 692, 72
Fan, Y.-Z., Zhang, B.-B., Xu, D., Liang, E.-W., & Zhang, B. 2011, ApJ, 726, 32
Gao, S., Asano, K., & Meszaros, P. 2012, ArXiv e-prints
Ghisellini, G., Ghirlanda, G., & Tavecchio, F. 2007, MNRAS, 375, L36
Guetta, D., & Della Valle, M. 2007, ApJ, 657, L73
Gupta, N., & Zhang, B. 2007, Astroparticle Physics, 27, 386
Karle, A., & for the IceCube Collaboration. 2010, ArXiv e-prints
Katz, B., Budnik, R., & Waxman, E. 2010, ApJ, 716, 781
Katz, B., Sapir, N., & Waxman, E. 2011, ArXiv e-prints
Katz, U. F. 2006, Nuclear Instruments and Methods in Physics Research A, 567, 457
Kneiske, T. M., Bretz, T., Mannheim, K., & Hartmann, D. H. 2004, A&A, 413, 807
Liang, E., Zhang, B., Virgili, F., & Dai, Z. G. 2007, ApJ, 662, 1111
Lien, A., & Fields, B. D. 2009, J. Cosmology Astropart. Phys., 1, 47
Madau, P., della Valle, M., & Panagia, N. 1998, MNRAS, 297, L17
Mazzali, P. A., Deng, J., Nomoto, K., et al. 2006, Nature, 442, 1018
Mirabal, N., Halpern, J. P., An, D., Thorstensen, J. R., & Terndrup, D. M. 2006, ApJ, 643, L99
Murase, K. 2008, Phys. Rev. D, 78, 101302
Murase, K., Ioka, K., Nagataki, S., & Nakamura, T. 2006, ApJ, 651, L5
—. 2008, Phys. Rev. D, 78, 023005
Murase, K., Thompson, T. A., Lacki, B. C., & Beacom, J. F. 2011, Phys. Rev. D, 84, 043003
Nakar, E., & Sari, R. 2010, ApJ, 725, 904
Ofek, E. O., Fox, D., Cenko, S. B., et al. 2012, ArXiv e-prints
Roming, P. W. A., Pritchard, T. A., Prieto, J. L., et al. 2012, ApJ, 751, 92
Smith, N., Chornock, R., Silverman, J. M., Filippenko, A. V., & Foley, R. J. 2010, ApJ, 709, 856
Soderberg, A. M., Kulkarni, S. R., Nakar, E., et al. 2006, Nature, 442, 1014
Soderberg, A. M., Berger, E., Page, K. L., et al. 2008, Nature, 453, 469
Soderberg, A. M., Chakraborti, S., Pignata, G., et al. 2010, Nature, 463, 513
Starling, R. L. C., Wiersema, K., Levan, A. J., et al. 2011, MNRAS, 411, 2792
Stoll, R., Prieto, J. L., Stanek, K. Z., et al. 2011, ApJ, 730, 34
Toma, K., Ioka, K., Sakamoto, T., & Nakamura, T. 2007, ApJ, 659, 1420
Vergani, S. D., D'Avanzo, P., Levan, A. J., et al. 2010, GRB Coordinates Network, 10512, 1
Wang, X.-Y., & Dai, Z.-G. 2009, ApJ, 691, L67
Wang, X.-Y., Li, Z., Waxman, E., & Mészáros, P. 2007, ApJ, 664, 1026
Waxman, E., & Bahcall, J. 1997, Physical Review Letters, 78, 2292
Waxman, E., Mészáros, P., & Campana, S. 2007, ApJ, 667, 351
Weaver, T. A. 1976, ApJS, 32, 233